NASA
Technical
Paper
2552

April 1986

Consideration of Some Factors Affecting Low-Frequency Fuselage Noise Transmission for Propeller Aircraft

John S. Mixson and
Louis A. Roussos

NASA

NASA
Technical
Paper
2552

1986

Consideration of Some Factors Affecting Low-Frequency Fuselage Noise Transmission for Propeller Aircraft

John S. Mixson and
Louis A. Roussos

Langley Research Center
Hampton, Virginia

National Aeronautics
and Space Administration

**Scientific and Technical
Information Branch**

INTRODUCTION

Propeller noise transmitted through the aircraft fuselage sidewall is an important contribution to the interior noise environment of many aircraft. Understanding this noise transmission is important for efficient prediction and control of cabin and cockpit noise. However, substantial research conducted on fuselage noise transmission (ref. 1) has indicated that areas of disagreement exist between measured and predicted transmission at low frequency (refs. 1 and 2). The sources of this disagreement have not been adequately explained at present, and the study of possible sources provides the subject of this paper.

The nature of the disagreement between measured and calculated noise transmission for an aircraft sidewall is illustrated in figure 1. The measured results, represented by the circular symbols, were obtained during ground tests of a light aircraft with propellers and engines operating (ref. 3). Sidewall noise reduction (NR) was determined by subtracting the cabin noise level SPL_i from the propeller noise level on the fuselage surface SPL_o. The propeller noise was measured at a position in the propeller plane where the noise level is expected to be maximum, and the cabin noise was measured in the propeller plane approximately 12 in. from the sidewall. Noise reduction was determined only at the propeller blade passage frequency and associated harmonics; operation at several engine rotational speeds resulted in the distribution of data points shown in figure 1. The overall trend of the data indicates a minimum NR at frequencies from 400 to 600 Hz and an increasing NR for both higher and lower frequencies. The transmission loss (TL) curve in figure 1 represents a first attempt to predict the measured results. Figure 1 shows that the calculated TL and the measured NR have similar trends at the higher frequencies but diverging trends at the lower frequencies. The focus of this paper is the identification of factors that might explain this divergence of trends and a simplified analysis of the effects of these factors on the trend.

An improved understanding of the factors affecting the low-frequency trends is of general interest for several reasons. First, cabin noise levels in propeller aircraft are often dominated by the low-frequency propeller tones. Thus, additional insight into the parameters affecting low-frequency noise transmission loss may be useful in the design and application of noise control methods to achieve passenger acceptance. Second, laboratory transmission-loss testing using standard methods of the American Society for Testing and Materials (ASTM) is frequently used to evaluate aircraft sidewalls and acoustic treatment. Results show that the measured TL in the laboratory usually follows the trend of TL shown in figure 1. Therefore, explanation of the low-frequency trends could form the basis of new laboratory test techniques or new methods for extrapolation of laboratory TL results to aircraft conditions. Third, the trend of the figure 1 data has also been observed for propeller aircraft in flight and for laboratory tests using simulated propeller noise. Improvement of existing theoretical methods for the aforementioned experimental conditions requires that only essential factors be included within the method and that nonessential factors, which serve only to increase the mathematical complexity, be omitted.

The factors considered in this paper are as follows: (1) the difference between noise reduction (NR) and transmission loss (TL); (2) the incidence angle of the noise source; (3) the plate structural dynamic characteristics; (4) absorption in the receiving space; and (5) the effect of a nonuniform source field. The purpose of this

paper is to identify the effects of these factors on the trends shown in figure 1 using simplified analysis methods.

In the development of the equations presented in the body of this report, three features were noted that are of interest beyond the main objectives of the report, and they are discussed in appendixes A, B, and C.

SYMBOLS AND ABBREVIATIONS

A,B,C	coefficients of plate response
b	rate of decay of nonuniform pressure
b_o	normalized rate of decay
c	sound speed
c_p	flexural wave speed in plate
D	plate stiffness parameter
D_p	propeller diameter
d	plate damping force coefficient
f	frequency, Hz
f_c	coincidence frequency, Hz
f(x)	distribution function of nonuniform pressure
H_0^2	Hankel function of the second kind
i	complex index, $\sqrt{-1}$
k	acoustic wave number
k_0	normalized wave number
k_1	plate wave number
ℓ	transform variable
m	plate mass
NR	noise reduction
P	general acoustic amplitude
P_f	factor for nonuniform transmission
P_i, P_r, P_t	incident, reflected, and transmitted amplitudes, respectively, of acoustic pressures

P_m magnitude of nonuniform distribution

p_i, p_r, p_t incident, reflected, and transmitted acoustic pressures, respectively

$p(x)$ nonuniform incident pressure distribution

r radius

SPL_D incident wave pressure reflection factor (SPL) and difference (D) between noise reduction and transmission loss

SPL_o, SPL_i sound pressure levels measured outside and inside aircraft, respectively

TL transmission loss

t time, sec

W amplitude of plate deflection

w plate deflection

$\bar{w}$ transform of plate deflection w (see eq. 24(a))

x, y, z geometric coordinates

x_o dummy coordinate in x-direction

Z_{plate} plate mechanical impedance (see eqs. (8) and (9))

α absorption coefficient

$\delta(0)$ Dirac delta function

ζ plate damping ratio

η dummy variable of integration

θ angle of incident plane wave

λ_p plate wavelength

ρ density of acoustic medium

ω circular frequency, rad/sec

ω_c coincidence frequency, rad/sec

∇^4 $= \dfrac{\partial^4}{\partial x^4} + 2\dfrac{\partial^4}{\partial x^2 \partial y^2} + \dfrac{\partial^4}{\partial y^4}$

A dot over a quantity indicates a derivative with respect to time.

NOISE REDUCTION FOR INCIDENT PLANE WAVES

The difference between noise reduction and transmission loss is discussed in this section using acoustic plane waves and an infinite uniform plate. The factors of interest are the definitions of NR and TL, sound incidence angle, plate structural properties, frequency, and absorption. The geometry is shown in figure 2. The acoustic pressure in the incident, reflected, and transmitted waves is, respectively,

$$p_i = P_i \exp[ik(x \cos\theta + y \sin\theta - ct)] \tag{1a}$$

$$p_r = P_r \exp[ik(y \sin\theta - x \cos\theta - ct)] \tag{1b}$$

$$p_t = P_t \exp[ik(x \cos\theta + y \sin\theta - ct)] \tag{1c}$$

The plate motion is governed by the plate equation

$$D\nabla^4 w + d\dot{w} + m\ddot{w} = (p_i + p_r - p_t)_{x=0} \tag{2}$$

If the pressures are substituted into equation (2), along with the expression for plate displacement w,

$$w = W \exp[i(yk \sin\theta - \omega t)] \tag{3}$$

the result is

$$(Dk^4 \sin^4\theta - i\omega d - m\omega^2)W = P_i + P_r - P_t \tag{4}$$

The boundary condition of displacement continuity uses the expression for acoustic particle displacement

$$\{iP \exp[ik(x \cos\theta + y \sin\theta - ct)]\}/\rho kc^2 \tag{5}$$

When applied on the transmitted side of the plate, this results in

$$P_t = -i\rho kc^2 W/\cos\theta \tag{6}$$

and on the incident side,

$$P_i - P_r = -i\rho kc^2 W/\cos\theta \tag{7}$$

Substituting equations (6) and (7) into (4) results in

$$\{Dk^4 \sin^4\theta - m\omega^2 - i[\omega d + (2\rho kc^2/\cos\theta)]\}W = 2P_i \tag{8}$$

or, for brevity,

$$\{Z_{plate}\}W = 2P_i \tag{9}$$

Noise reduction is obtained from these equations as follows. Noise reduction is defined as the difference between the noise levels on the incident and transmitting sides of the plate. The incident noise level is determined at the plate surface in order to provide similarity with the aircraft situation. For aircraft, the outside noise level is usually the total noise measured at the fuselage surface because incident and reflected components are difficult, if not impossible, to separate and because measurements can be made on the fuselage surface. Therefore, noise reduction is given as

$$NR = SPL_o - SPL_i \tag{10a}$$

$$= 20 \log \left| \frac{p_{total}}{p_{ref}} \right| - 20 \log \left| \frac{p_t}{p_{ref}} \right| \tag{10b}$$

$$= 20 \log \left| \frac{p_{total}}{p_t} \right| \tag{10c}$$

where

$$|p_{total}| = |p_i + p_r| \tag{11}$$

$|p_{ref}|$ acoustic reference pressure

$|p_t|$ transmitted pressure

Noise reduction can be related to transmission loss (TL) using equation (10c) and the definition

$$TL = 10 \log \left| \frac{p_i}{p_t} \right|^2 = 20 \log \left| \frac{p_i}{p_t} \right| \tag{12}$$

to obtain

$$NR = TL + 20 \log \left| \frac{p_{total}}{p_i} \right| = TL + SPL_D \tag{13a}$$

and

$$SPL_D = NR - TL = 20 \log \left| \frac{p_{total}}{p_i} \right| \tag{13b}$$

Equation (13a) is useful because it relates NR, the quantity that characterizes aircraft noise transmission, with TL, the quantity measured in the laboratory. Expressions for TL and SPL_D in terms of plate and acoustic properties can be obtained using equations (1) to (12). For TL, W can be obtained from equation (8) and substituted into equation (6); then the definition of equation (12) can be used to obtain

$$TL = 10 \log \left[\left(1 + \frac{d \cos \theta}{2\rho c} \right)^2 + \left(\frac{m\omega \cos \theta}{2\rho c} \right)^2 \left(1 - \frac{D\omega^2 \sin^4 \theta}{mc^4} \right)^2 \right] \tag{14}$$

With an appropriate definition of terms, the TL given by equation (14) can be shown to reduce to previously derived results (ref. 4).

In equation (14) the damping ratio ζ and the coincidence frequency ω_c can be introduced, where

$$\zeta = d \Big/ \left(2k^2 \sin^2 \theta \sqrt{mD} \right) \tag{15}$$

and

$$\omega_c^2 = mc^4/D \tag{16}$$

to obtain

$$\left|\frac{P_i}{P_t}\right|^2 = \left(1 + 2\zeta \frac{\omega^2}{\omega_c^2} \sin^2\theta \frac{m\omega_c \cos\theta}{2\rho c}\right)^2 + \left(\frac{m\omega_c \cos\theta}{2\rho c} \frac{\omega}{\omega_c}\right)^2 \left(1 - \frac{\omega^2}{\omega_c^2} \sin^4\theta\right)^2 \tag{17}$$

which gives TL in terms of nondimensional parameters. As shown by equation (13b), SPL_D requires a relation between p_i and p_{total}, where p_{total} is given by equation (11). The relation can be obtained by combining equations (1) and (9), which results in

$$SPL_D = 20 \log\left(2\left|1 + \frac{i\rho c\omega}{Z_{plate} \cos\theta}\right|\right) \tag{18}$$

Equations (17) and (18), with (8) and (13a), show that NR is a complicated function of the plate parameters (ζ, ω_c, and m), the acoustic parameters (θ and ρc), and the circular frequency (ω). The sensitivity of NR to variations of the plate and acoustic parameters can be evaluated using these equations in order to obtain guidance for prediction of NR for comparison with the aircraft results shown in figure 1.

The variation of TL with frequency ratio is shown in figure 3 for several values of incidence angle and for a 0.040-in-thick aluminum plate vibrating in air. The solid curves indicate TL values calculated using the complete equation (17). These curves show that TL is very sensitive to incidence angle and frequency ratio. The symbols shown in figure 3 represent TL values obtained using the simplified expression

$$TL = 10 \log\left[1 + \left(\frac{m\omega_c}{2\rho c}\right)^2 \left(\frac{\omega}{\omega_c}\right)^2 \cos^2\theta\right] \tag{19}$$

obtained from equation (17) by setting plate damping and stiffness to 0 and retaining only plate mass. The figure shows that results from equation (19) are in close agreement with the more complete equation (17) for a range of frequencies whose upper limit depends on incidence angle θ. Since the coincidence frequency ω_c for the aircraft structure shown in figure 1 (0.040-in-thick aluminum skin) is large compared with the frequency range of interest, the results of figure 3 indicate that the simpler equation (19) can be used.

The expression for SPL_D was also simplified by setting plate stiffness D and damping ζ to 0 in equation (8). Combining equations (8) and (18) results in

$$SPL_D = 20 \log\left(\frac{2\left\{\left[2 + \left(\frac{m\omega \cos\theta}{\rho c}\right)^2\right]^2 + \left(\frac{m\omega \cos\theta}{\rho c}\right)^2\right\}^{1/2}}{4 + \left(\frac{m\omega \cos\theta}{\rho c}\right)^2}\right) \tag{20}$$

Figure 4 presents the variations of SPL_D with θ and frequency obtained from using equation (20). This figure shows that SPL_D is sensitive to incidence angle for large angles but is not very sensitive to frequency for $\theta = 0°$.

Because NR is sensitive to incidence angle, it is appropriate to examine the incidence angles associated with the propeller data of figure 1 and to consider how to include them in the calculation of NR. Impinging noise from a propeller has been measured using microphones flush mounted in the fuselage sidewall (ref. 3). Examination of phase data for pairs of microphones led to the impingement angle model shown in figure 5. According to this model the measured phase data for each pair of microphones could be interpreted in terms of a plane wave incident on the sidewall at angle θ. The incidence angles determined for that test are shown in figure 5 for positions along the fuselage length. The aircraft used to obtain the incidence angle data of figure 5 is the same aircraft used to obtain the sidewall transmission data shown in figure 1. Incidence angles obtained from figure 5 are plotted in figure 6 as a function of position along the fuselage sidewall x/D_p. To calculate NR at all positions, the continuous curve shown in the figure has been fitted (approximately) to the data. These values of θ are used in equations (13a), (19), and (20) (along with structural and acoustic values for a 0.040-in-thick aluminum plate in air) to calculate noise reduction.

The noise reduction results are shown in figure 7(a) for two frequencies. The exterior propeller noise levels obtained in the tests that led to the incidence angle data of figure 6 are shown in figure 7(b). Figure 7(a) shows that noise reduction varies by about 6 dB for the range of x/D_p shown. Calculation of interior noise level would require combining NR with the exterior noise levels shown in figure 7(b). Both the noise reduction and the exterior level are higher near the propeller plane ($x/D_p = 0$) and lower at the aft position (toward $x/D_p = -1.2$). If the fuselage at each value of x/D_p could be assumed to behave as an infinite flat plate, then a strip theory could be used to calculate the transmission through the structure at each x/D_p. In this case the variations of NR and SPL_o shown in figure 7 would suggest that noise transmitted to the interior would be nearly as much at aft cabin positions, where the exterior noise level is lower, as at forward positions. (Most sidewall treatments are heavier near the propeller plane in current aircraft.) The development of a theory to account for variations of sidewall noise reduction NR and propeller noise source SPL is beyond the scope of this paper.

For a comparison with measured results, the NR calculated for $x/D_p = 0$ and for the condition where the transmitted wave is totally absorbed is shown in figure 8 as $(NR)_{\alpha=1}$. The overall trend of calculated NR with frequency is about the same as for TL (fig. 1), but the values are larger so that noise reduction at frequencies above about 400 Hz lies along the upper edge of the band of data. At lower frequencies NR is closer to the data than TL is, but there is still a substantial difference from the data; also, the trend of the theory is still different from the data in that the predicted values decrease with decreasing frequency whereas the measured values increase.

Also shown in figure 8 is a curve labeled "NR(α)." This curve was calculated to determine whether absorption on the transmitted side of the plate would change the trend of the predicted NR at low frequencies. For the model of figure 2, the transmitted plane wave propagates completely away from the plate and the effective

absorption coefficient α is 1. As an approximation, the noise level on the transmitted side of the plate is corrected using the relation

$$SPL(\alpha) = (SPL)_{\alpha=1} - 10 \log \alpha \tag{21}$$

The level $(SPL)_{\alpha=1}$ is determined from the model of figure 2; and since α is between 0 and 1, the corrected value $SPL(\alpha)$ will be higher than $(SPL)_{\alpha=1}$. Using the definition of noise reduction, equation (10a), and equation (21) for the transmitted noise SPL_i, it can be shown that

$$NR(\alpha) = (NR)_{\alpha=1} + 10 \log \alpha \tag{22}$$

where $NR(\alpha)$ is the noise reduction for various α and $(NR)_{\alpha=1}$ is the noise reduction for $\alpha = 1$. Equation (22) shows that when absorption is less than 1, the noise reduction is decreased. The absorption values shown in figure 9 were used to calculate the effect, and the result is shown as $NR(\alpha)$ in figure 8. It is apparent that the inclusion of absorption did not improve the agreement between predicted and measured trends at low frequency.

The results obtained using the preceding model of an infinite plate with plane acoustic waves indicate that the magnitude of the predicted noise transmission was sensitive to the definition of TL and NR, the sound incidence angle, cabin absorption, and the plate dynamic properties. However, the trend of predicted NR with frequency remained the same and was still in disagreement with propeller test data. This model assumed that the incident sound had the same magnitude at all positions on the plate. Figure 7 indicated, however, that the incident sound level due to a propeller is not constant over the fuselage but has a larger magnitude near the plane of the propeller. The effect of this nonuniformity of the propeller noise field on the low-frequency trend of predicted noise transmission is examined in the next section.

NONUNIFORM INCIDENT PRESSURE

The characteristics of the propeller noise incident on an aircraft fuselage are different from the characteristics of the plane acoustic wave used in the preceding analysis and of the reverberant field used in standard laboratory transmission-loss tests. One of the characteristics of propeller noise is the higher loads near the plane of rotation of the propeller, as indicated in figure 7(b). The following simplified analysis is intended to explore the nature and magnitude of the effects associated with concentration of the incident noise in a localized area.

The analysis is based on the simplified plate equation

$$D \frac{d^4 w}{dx^4} - m\omega^2 w(x) = P_m f(x) \tag{23}$$

To obtain this equation, plate damping and the effects of acoustic radiation on the plate motion have been neglected, the incident pressure $P_m f(x)$ has been taken to be normally incident and independent of the plate coordinate y (see fig. 10), and the motion is simple harmonic in time. The solution is carried out using the transforms

$$\bar{w}(\ell) = \int_{-\infty}^{\infty} w(x)\, e^{-i\ell x}\, dx \tag{24a}$$

and

$$w(x) = \frac{1}{2\pi} \int_{-\infty}^{\infty} \bar{w}(\ell)\, e^{i\ell x}\, d\ell \tag{24b}$$

Substitution into equation (23), inversion of the solution of the resulting equation, and integration leads to the solution

$$w(x) = \frac{iP}{4k_0^3}\left[e^{ik_0 x} \int_{-\infty}^{\infty} f(\eta)\, e^{-ik_0\eta}\, d\eta + ie^{-k_0 x} \int_{-\infty}^{\infty} f(\eta)\, e^{k_0\eta}\, d\eta\right] \tag{25}$$

where $k_0^4 = m\omega^2/D$ and the solution applies in the range $x - \eta > 0$. Further solution requires specification of the incident pressure distribution $f(\eta)$. As a check, this equation can be shown to reduce to a solution given in reference 5 for the case $f(\eta) = \delta(0)$, with $x > 0$, where $\delta(0)$ is the Dirac delta function. To investigate a range of distributions, $f(\eta)$ is taken in the form

$$f(\eta) = e^{-b|\eta|} \tag{26}$$

Substitution into equation (25) leads to the solution

$$w(x) = \frac{iP}{4k_0^3}\left(Ae^{-b|x|} + Be^{ik_0|x|} + Ce^{-k_0|x|}\right) \tag{27}$$

where

$$A = \frac{-4ik_0^3}{b^4 - k_0^4} \qquad B = \frac{2b}{b^2 + k_0^2} \qquad C = \frac{2ib}{b^2 - k_0^2} \tag{28}$$

This plate motion can be used to find the transmitted acoustic pressure using the relation

$$p(x,z) = -\frac{1}{2} i\rho\omega^2 \int_{-\infty}^{\infty} w(x_o)\, H_0^2(kr)\, dx_o \tag{29}$$

where $p(x,z)$ is the transmitted pressure, $w(x_o)$ is the plate motion, H_0^2 is the Hankel function of the second kind, and $r^2 = (x - x_o)^2 + z^2$. Substitution of w from equation (27) into equation (29) leads to integrals for which general solutions have not yet been found. A closed-form solution has been found only for the position $x = z = 0$ on the transmitted side of the plate. This position is directly opposite the maximum of the incident pressure and can be expected to have the maximum transmitted pressure. For this case the solution, written in terms of noise reduction NR, is

$$NR = 20 \log \left| \frac{P}{p(0,0)} \right| = 20 \log \frac{m\omega}{\rho c} - 20 \log |P_f| \tag{30}$$

where

$$P_f = \frac{-i + \frac{2}{\pi} \ln\left(b_o k_1 + \sqrt{1 + b_o^2 k_1^2}\right)}{\left(b_o^4 - 1\right)\sqrt{1 + b_o^2 k_1^2}} + \frac{i + \frac{1}{\pi} \ln\left(k_1 - \sqrt{k_1^2 - 1}\right) b_o}{\left(b_o^2 + 1\right)\sqrt{k_1^2 - 1}}$$

$$+ \frac{\frac{i}{2} - \frac{1}{\pi} \ln\left(k_1 + \sqrt{k_1^2 + 1}\right) b_o}{\left(b_o^2 - 1\right)\sqrt{k_1^2 + 1}} \tag{31}$$

and

$$b_o = b/k_0 \qquad k_1 = k_0/k \qquad (0 < k < k_0) \tag{32}$$

As indicated by equation (26), b is the rate of decrease of the incident pressure in the x-direction. If the incident pressure is a constant, then $b = 0$, $b_o = 0$, and equation (30) reduces to

$$NR = 20 \log \frac{m\omega}{\rho c} \tag{33}$$

Equation (33) can be understood by reference to equations (13a), (19), and (20). From equation (20), a wave normally incident on a plate with a large value of $m\omega/\rho c$ will result in

$$SPL_D = 20 \log 2 \tag{34}$$

Combining this result with equations (13a) and (19) leads to

$$NR = 10 \log[1 + (m\omega/2\rho c)^2] + 20 \log 2 \tag{35}$$

A rederivation of equation (13a) shows that the term "1" in equation (35) results from the effect of acoustic radiation on plate motion. Neglect of acoustic radiation (neglecting the "1") reduces equation (35) to equation (33). Thus, equation (33) represents the noise reduction for a normally incident wave on a plate having high resistance $m\omega/\rho c$, derived without the effect of acoustic radiation on the plate motion. It follows that the term "$-20 \log |P_f|$" in equation (30) is a correction term for the effect of a nonuniform incident pressure.

Equation (27) shows that the plate motion has three components: a component that decays at the same rate as the incident pressure, $e^{-b|x|}$; a term that decays at a rate determined by the plate wave number k_0, $e^{-k_0|x|}$; and a wave term, $e^{ik_0|x|}$. Equation (31) shows that the correction term depends on the three parameters b_o, k_1, and their product $b_o k_1$. From equation (32), b_o is the ratio of acoustic wave number to plate wave number, and $b_o k_1$ is the ratio of incident pressure decay rate b to acoustic wave number k. Thus, the correction for nonuniform incident pressure depends not only on the incident pressure distribution but also on the plate dynamics through k_0, and also on the acoustic dynamics through k.

The plate and acoustic dynamic parameters enter through the relations

$$k_0 = 2\pi/\lambda_p = \omega/c_p \tag{36a}$$

$$k_0^4 = m\omega^2/D \tag{36b}$$

$$k = \omega/c \tag{36c}$$

$$f_c = \left(c^2\sqrt{m/D}\right)/2\pi \tag{36d}$$

The coincidence frequency f_c is the frequency at which the singularity occurs in P_f, as shown in equation (31). This frequency corresponds to the coincidence frequency of reference 4. The variation of noise reduction with frequency is shown in

figure 11 for a 0.040-in-thick aluminum plate vibrating in air. Figure 11 shows that for small values of b_o, the noise reduction has small values at low frequency and increases with increasing frequency, and the curve resembles those for incident plane waves such as those shown in figure 3. Small values of b_o correspond to incident pressure that has nearly uniform distribution and decays slowly compared with the plate decaying component. For larger values of b_o, the shape of the curves changes and a trend of increasing NR with decreasing frequency appears. The values of noise reduction also increase to quite large values that are not usually associated with a plate of only 0.040 in. thickness. This behavior of NR at low frequency is associated with the concentration of the incident pressure over a small region, resulting in a large value of b compared with the plate parameter k_0, and is distinct from the low-frequency stiffness-controlled behavior (ref. 4) usually associated with boundary-condition effects on a stiff plate.

The above equations have been used for the prediction of aircraft results such as those shown in figure 1. In this calculation, equation (30) was modified to account (approximately) for acoustic radiation effects by the change

$$20 \log \frac{m\omega}{\rho c} \rightarrow 20 \log\left(1 + \frac{m\omega}{\rho c}\right) \tag{37}$$

The form of b_o used for this calculation was based on measured structural dynamic properties of the aircraft presented in reference 6 and on observed acceleration behavior of the sidewall components (ref. 7). It has been observed (for example, see ref. 7) that the accelerations of fuselage skin panels at low frequencies are about the same as the accelerations of the adjacent stiffener members. Based on this observation it is assumed that panels and stiffeners have the same vibrational wavelength. Modal distributions measured primarily on stiffeners are presented in reference 6 for modal frequencies from 61 to 189 Hz. Observations of the wavelengths associated with these modes suggest that the measured wavelengths can be represented approximately by the relation

$$\lambda_p = 26/\sqrt{f} \tag{38}$$

Examination of the propeller noise field for tests such as those leading to the data in figure 1 suggests that the exponential distribution (eq. (26)) is a rough approximation to the propeller data for $b = 2.42$. The parameter b_o was therefore represented by

$$b_o = b\lambda_p/2\pi = 2.42 \frac{26}{2\pi\sqrt{f}} \tag{39}$$

With these approximations, equations (30) and (31) were used to predict noise reduction. Figure 12 shows that the noise reduction for a nonuniform source (NR_{NU}) is within the range of the test data at frequencies below about 300 Hz, and comparison with figure 8 shows that NR_{NU} is substantially larger in magnitude and has a different trend with frequency compared with predicted NR for a uniform incident field.

These results along with the results shown in figure 11 indicate that the nonuniformity of the incident field can have a substantial effect on the predicted noise reduction, and the effects tend to bring predicted results into closer agreement with trends of measured noise reduction at low frequencies for an aircraft with engines and propellers in operation.

CONCLUDING REMARKS

This paper presents an analysis of some factors that influence the noise transmission through an aircraft sidewall and evaluates the effects of the factors on differences between laboratory transmission loss (TL) results and propeller aircraft noise reduction (NR) results. The factors considered include the difference between TL and NR, incidence angles of the source noise, plate structural dynamic characteristics, absorption in the receiving space (aircraft cabin), and the effect of a nonuniform source noise distribution (representing a propeller noise field). Approximate analysis methods were used because the objective of this paper involved determination, in a qualitative sense, of the influence of the aforementioned factors on the trend of NR with frequency at low frequencies. A model consisting of acoustic plane waves incident on an infinite flat plate was used to evaluate TL versus NR, incidence angle, plate properties, and cabin absorption. The results indicate that these factors had significant effects on noise transmission but did not account for the divergence observed between measured and predicted trends of noise transmission at low frequencies.

The model used to evaluate the effect of nonuniform source noise distribution consisted of an infinite flat panel acted on by a (normal) pressure having an exponentially decaying magnitude along one coordinate and a constant value along the other. Results from the application of this model showed that transmitted noise was a complicated function of combined plate and acoustic parameters. In particular, the effect of the nonuniform distribution of incident noise was to change the trend of noise reduction at low frequency from decreasing to increasing with decreasing frequency, thus bringing the predicted trend into better agreement with the trend of measured results for a propeller aircraft. This phenomenon has not been reported previously and is entirely independent of low-frequency stiffness-controlled effects associated with boundary-condition effects on stiff plates. Estimated magnitudes of the effect for the airplane properties of interest indicated that noise transmission values were in the range of the measured results and were much higher (30 dB) than values usually associated with structures such as the aircraft sidewalls. In general, these results indicate that source noise distribution, as well as incidence or phase angle, has an important effect on noise transmission and should be included in analytical models for propeller aircraft.

NASA Langley Research Center
Hampton, VA 23665-5225
January 16, 1986

APPENDIX A

APPROXIMATE TL EQUATION

Approximate equations are frequently of use for the prediction of field-incidence transmission loss. The exact result is obtained by numerical integration over incidence angle of transmission expressions such as equation (14) or equation (19). The result of such an integration as described in reference 8 is shown in figure 13 as field-incidence mass law (TL_{field}) along with curves of TL for individual values of incidence angle. It has been observed (ref. 4) that the TL_{field} curve lies approximately parallel to and 5 dB below the curve for $\theta = 0°$. The simplified equation recommended by reference 4 is therefore

$$TL_{field} = (TL)_{\theta=0} - 5 \text{ dB} \tag{A1}$$

where normal incidence TL is found from

$$(TL)_{\theta=0} = 10 \log\left[1 + \left(\frac{m\omega}{2\rho c}\right)^2\right] \tag{A2}$$

These equations are restricted to values of $(TL)_{\theta=0}$ not less than 15 dB, and it can be seen that equation (A1) produces negative values of TL_{field} for small frequencies. Figure 13 shows also that the curve for TL_{field} lies between the TL curves for $\theta = 45°$ and 60°, and somewhat closer to the curve for $\theta = 60°$. This observation suggests that an approximate formula could be obtained by using a single value of θ. Since mass law results are reasonably accurate for low frequency, use of equation (19) with $\theta = \theta_{field}$ is suggested:

$$TL_{field} = 10 \log\left[1 + \left(\frac{m\omega_c}{2\rho c}\right)^2 \left(\frac{\omega}{\omega_c}\right)^2 \cos^2\theta_{field}\right] \tag{A3}$$

Calculation shows that $\theta_{field} = 55°$ provides a reasonable fit of equation (A3) with the exact TL_{field} curve shown in figure 13. Equation (A3) is as easy to use as equations (A1) and (A2), does not produce negative values at any frequency, and is therefore proposed as an approximate equation for calculation of field-incidence transmission loss.

APPENDIX B

SURFACE REFLECTION CORRECTION

The relation between free-field incident source noise and sound pressure exerted on a structural surface in the noise field is of interest. For example, empirical methods for the prediction of propeller noise pressures on an aircraft fuselage (ref. 9) combine free-field propeller noise with an empirical reflection-correction factor based on measured results. The reflection correction used in reference 9 is shown in figure 14(a). The equations derived in the body of this report can be used to calculate the reflection effects. Specifically, the factor SPL_D as defined by equation (13b), which gives the ratio in decibels of total surface pressure to incident pressure, is the amount that would be added to incident SPL to obtain SPL on the surface. It is therefore directly comparable to the empirical reflection correction shown in figure 14(a).

Equation (18) shows that SPL_D is a function of frequency, acoustic impedance ρc, incidence angle θ, and plate dynamics through Z_{plate}. Values of SPL_D can be calculated using the simplified expression in equation (20), obtained by setting plate stiffness and damping to 0. Equation (20) can be evaluated in the limit as $m\omega$ becomes infinite to obtain $SPL_D = 6$ dB. This result applies for all angles of incidence and is a check of the validity of equation (20) since the same 6-dB pressure increase can be obtained by the method of images for the case of a rigid boundary. For a plate that is not rigid, however, the pressure reflection factor depends on the angle of incidence as well as on plate mass, frequency, and acoustic impedance ρc. Equation (20) has been evaluated for a 0.040-in-thick aluminum plate vibrating in air at sea level conditions. The results, shown in figure 4, indicate that the reflection factor is nearly 6 dB for near-normal incidence and most frequencies, but it decreases to 0 at 90° incidence. This result shows that the dynamics of the reflecting surface can have an important effect on the surface pressure since SPL_D is 6 dB for a rigid surface but is 0 for a nonrigid surface (at 90° incidence).

Values of SPL_D can be compared with the empirical curve in figure 14(a), but only qualitatively since the dynamics of the reflecting surface used to obtain the empirical curve are not known. Equation (20) gives SPL_D in terms of incidence angle, but the empirical reflection factors are presented in figure 14 as a function of normalized distance from the propeller plane, rather than incidence angle. To relate distance and incidence angles, measured results for apparent incidence directions and distance, shown in figure 6, are used. The curve in figure 6, which was calculated based on a point source, is used to interpolate between data points. This curve was used together with the factor SPL_D given by equation (20) to determine SPL_D as a function of position, x/D_p. The result is shown in figure 14(b) for comparison with the empirical values given by reference 9. Both the calculated and empirical curves have the same general character, having a maximum value near the propeller plane of rotation and reduced values with increasing distance from the propeller plane. This result suggests that the nonrigidity of the reflecting surface influenced the measured magnitude of the pressure increment due to reflection.

APPENDIX C

COMPOSITE CONSTRUCTION

The equations derived for the nonuniform incident pressure indicate that the noise transmission depends strongly on the interaction between the plate dynamics $\left(\text{through the factor } k_0 = \sqrt[4]{m\omega^2/D}\right)$ and the incident pressure (through the decay ratio factor b). Figure 11 shows that large increases of noise reduction occur with increases of $b_o = b/k_0$. This result suggests that stiffer plates, having a larger ratio of stiffness to mass D/m and therefore larger b_o, might transmit less noise than less stiff plates. Increased stiffness might be obtained by use of composites such as graphite-epoxy material in place of metal. Some previous studies (ref. 10) indicate that plates constructed of advanced composite materials, such as graphite fibers in an epoxy matrix, may have lower transmission loss than equivalent aluminum plates. Factors affecting the relative noise transmission include plate mass and stiffness and the characteristics of the incident sound. Previous studies used incident plane waves with uniform distribution over the plate. The equations derived in this paper use the equivalent of a normally incident wave with a magnitude that varies over the plate. These results suggest that composite panels might have a noise reduction benefit for localized noise sources, such as propellers.

REFERENCES

1. Mixson, John S.; and Powell, Clemans A.: Review of Recent Research on Interior Noise of Propeller Aircraft. AIAA-84-2349, Oct. 1984.

2. Mixson, John S.; Barton, C. Kearney; and Vaicaitis, Rimas: Investigation of Interior Noise in a Twin-Engine Light Aircraft. J. Aircr., vol. 15, no. 4, Apr. 1978, pp. 227-233.

3. Piersol, A. G.; Wilby, E. G.; and Wilby, J. F.: Evaluation of Aero Commander Propeller Acoustic Data: Taxi Operations. NASA CR-159124, 1979.

4. Beranek, Leo L., ed.: Noise and Vibration Control. McGraw-Hill Book Co., Inc., c.1971.

5. Junger, Miguel C.; and Feit, David: Sound, Structures, and Their Interaction. MIT Press, c.1972.

6. Geisler, D. L.: Experimental Modal Analysis of an Aero Commander Aircraft. NASA CR-165750, 1981.

7. Barton, C. K.; and Mixson, J. S.: Noise Transmission and Control for a Light Twin-Engine Aircraft. J. Aircr., vol. 18, no. 7, July 1981, pp. 570-575.

8. Mixson, John S.; Roussos, Louis A.; Barton, C. Kearney; Vaicaitis, Rimas; and Slazak, Mario: Laboratory Study of Add-On Treatments for Interior Noise Control in Light Aircraft. J. Aircr., vol. 20, no. 6, June 1983, pp. 516-522.

9. Prediction Procedure for Near-Field and Far-Field Propeller Noise. AIR 1407, Soc. Automot. Eng., Inc., May 1977.

10. Roussos, Louis A.; Grosveld, Ferdinand W.; Koval, Leslie R.; and Powell, Clemans A.: Noise Transmission Characteristics of Advanced Composite Structural Materials. AIAA-83-0694, Apr. 1983.

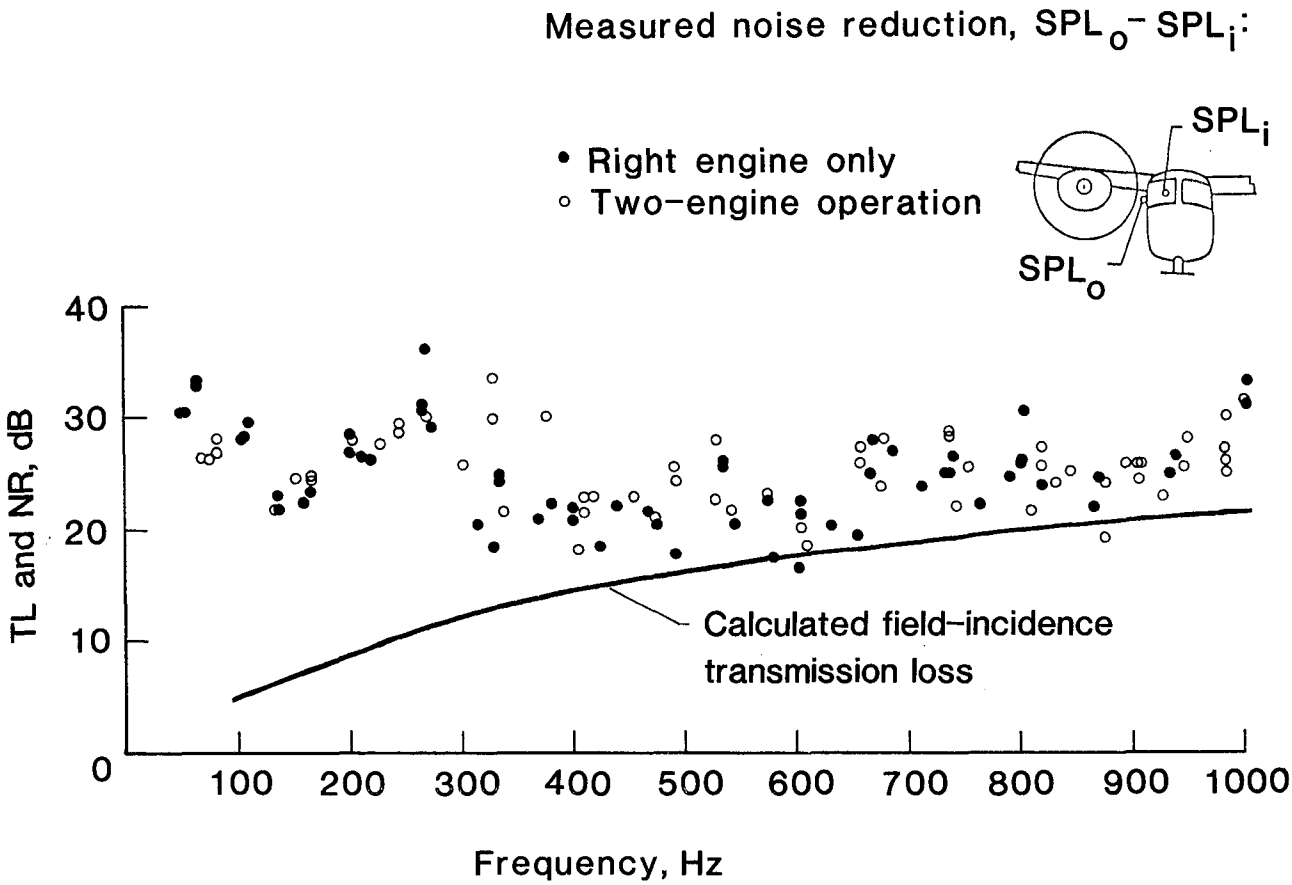

Figure 1.- Noise transmission from propeller tests and infinite panel theory.

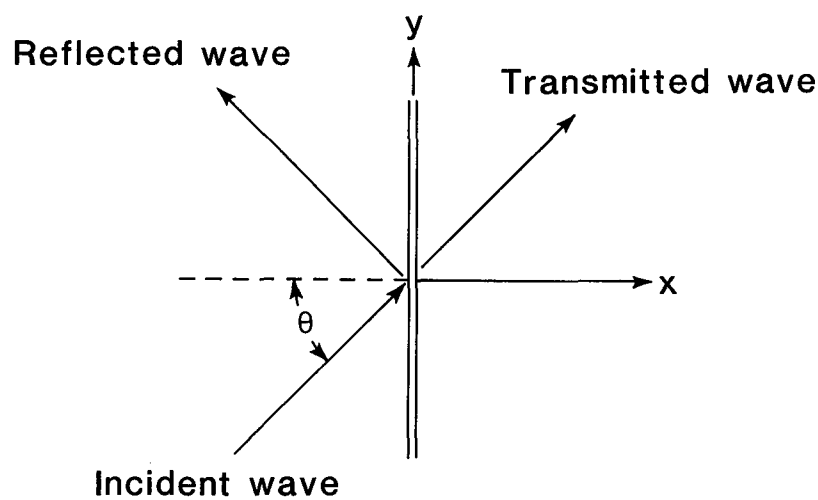

Figure 2.- Geometry of plane wave transmission.

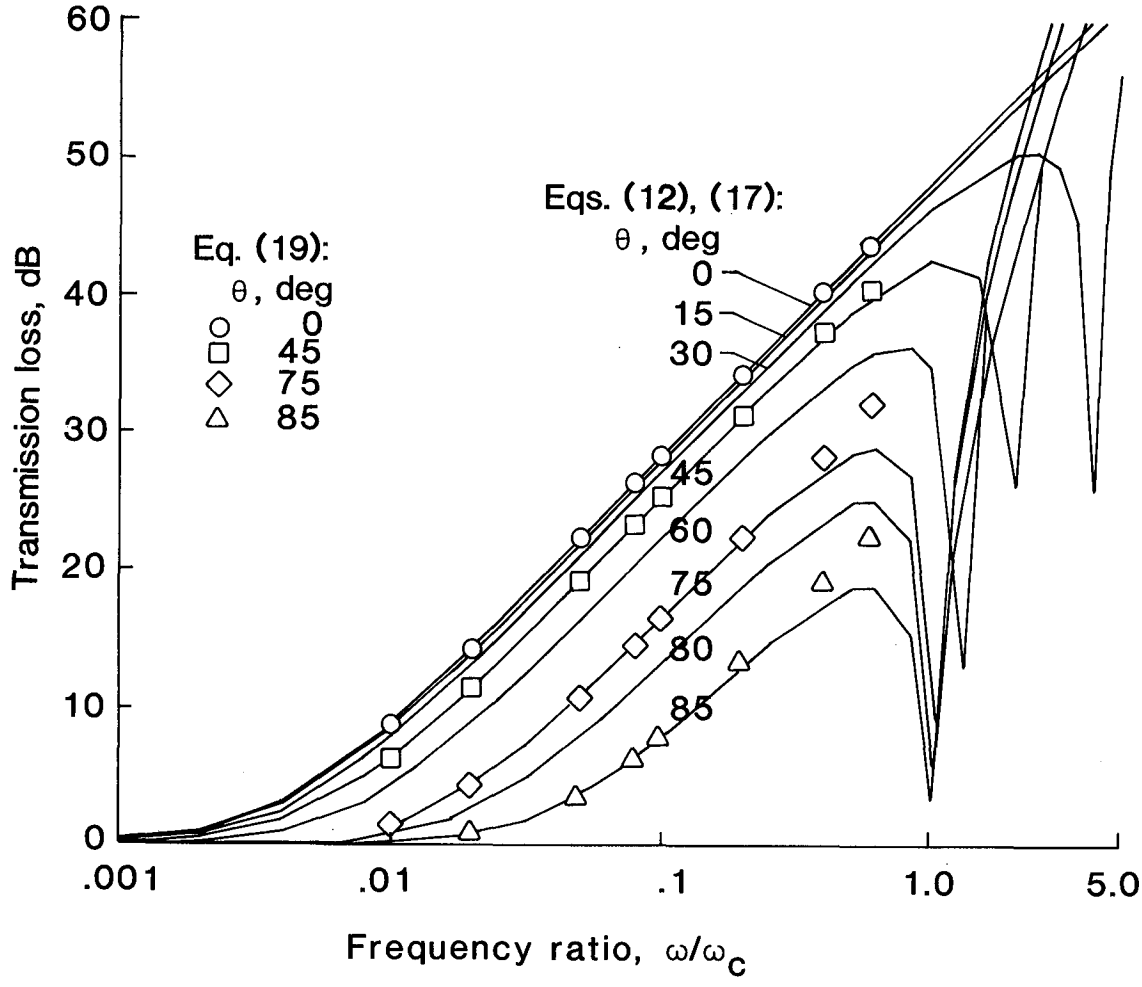

Figure 3.- Variation of transmission loss with frequency ratio for two calculation methods.

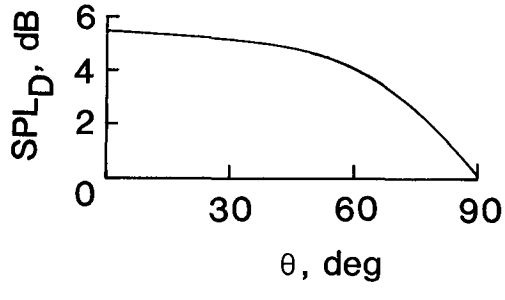

(a) Variation with incidence angle. f = 100 Hz.

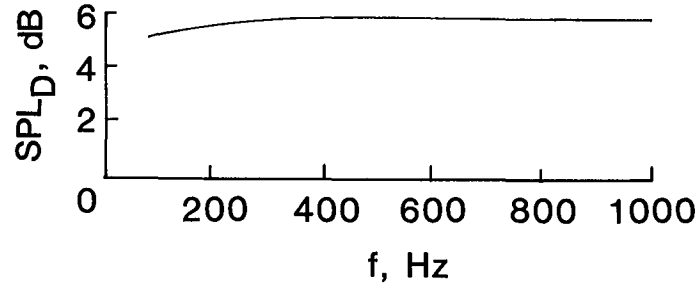

(b) Variation with frequency. θ = 0°.

Figure 4.- Difference between noise reduction and transmission loss. 0.040-in-thick aluminum plate; in air; SPL_D = NR - TL.

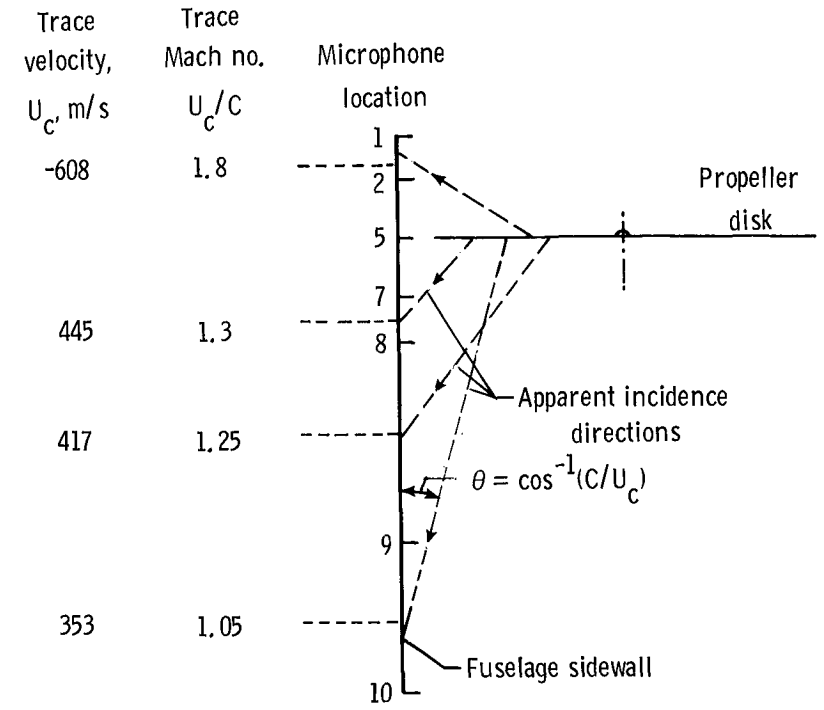

Figure 5.- Apparent incident angles for propeller noise on light aircraft fuselage. See reference 1.

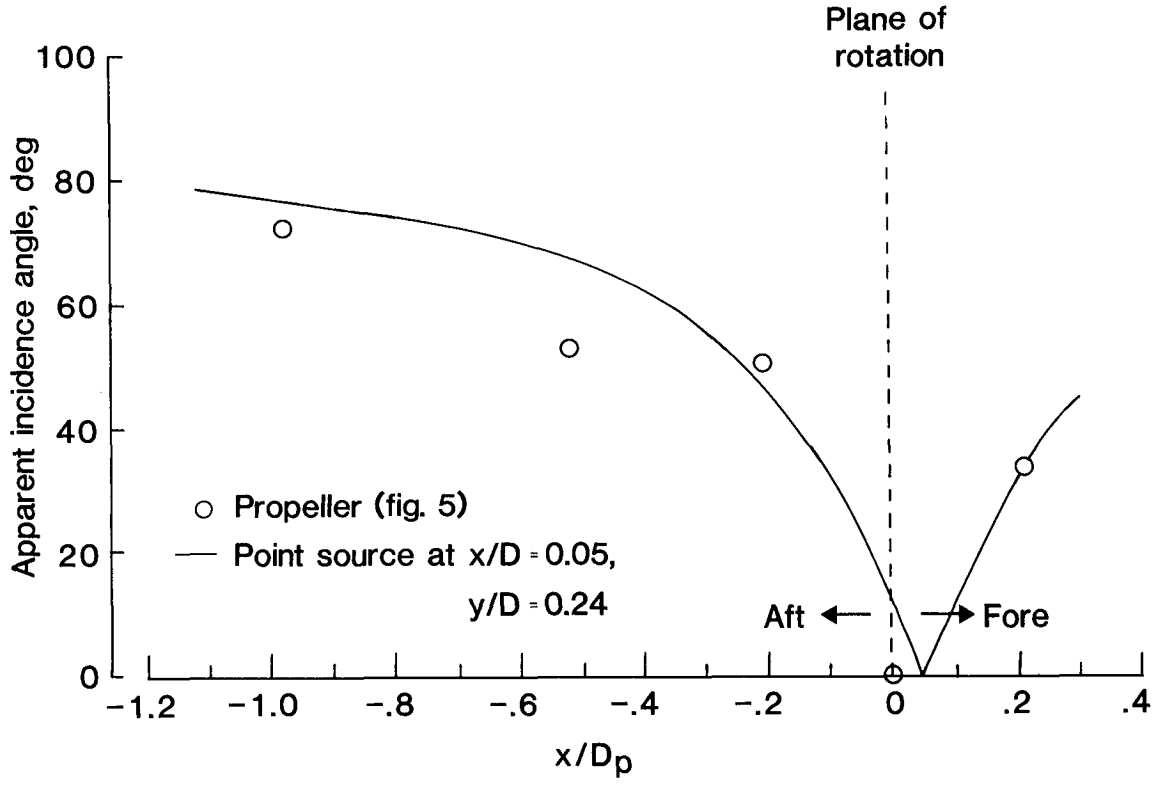

Figure 6.- Apparent incidence directions. $\theta = \frac{\tan^{-1}(x/D)}{y/D}$.

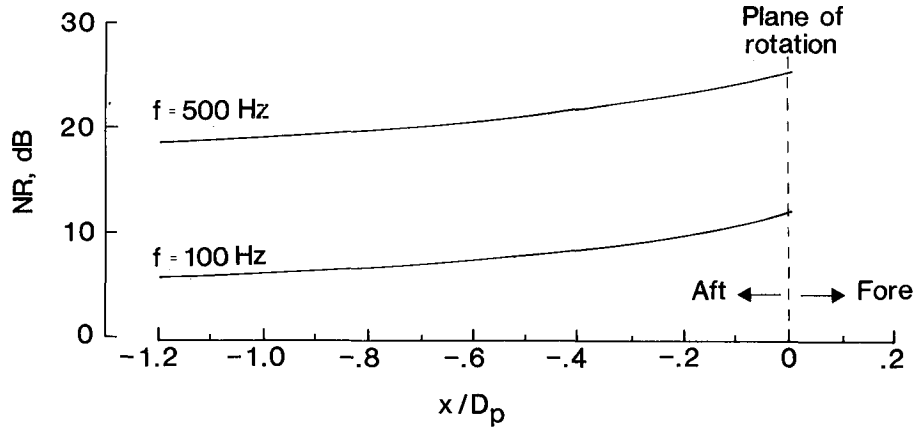

(a) Noise reduction (NR).

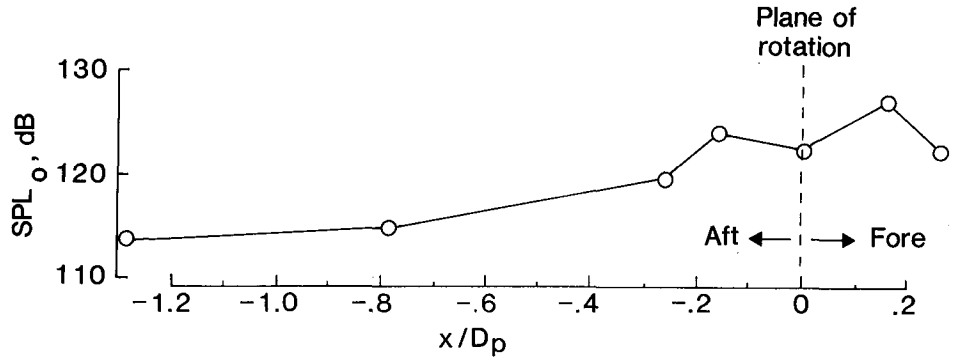

(b) Propeller exterior noise (SPL_o).

Figure 7.- Variation of source noise and sidewall transmission for propeller aircraft.

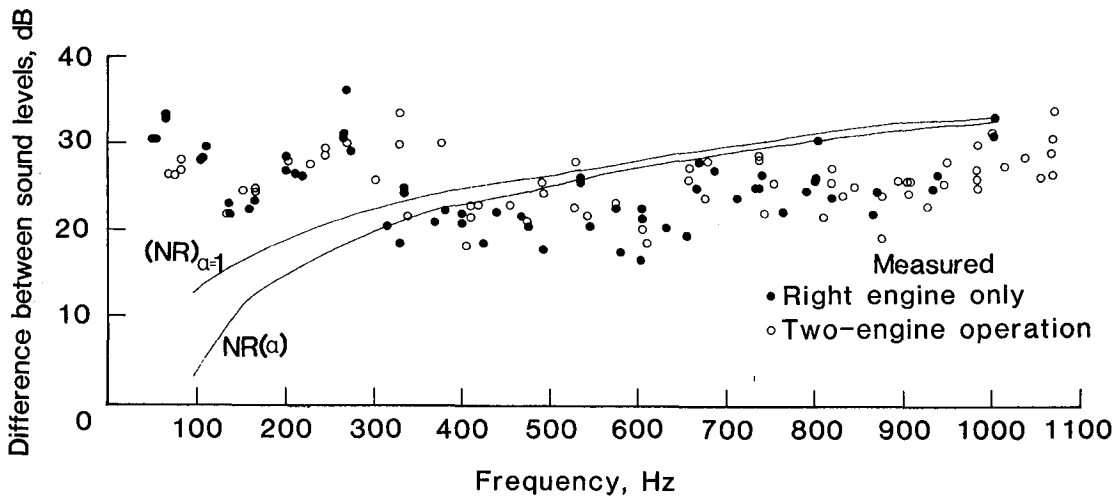

Figure 8.- Noise transmission from propeller tests and predictions.

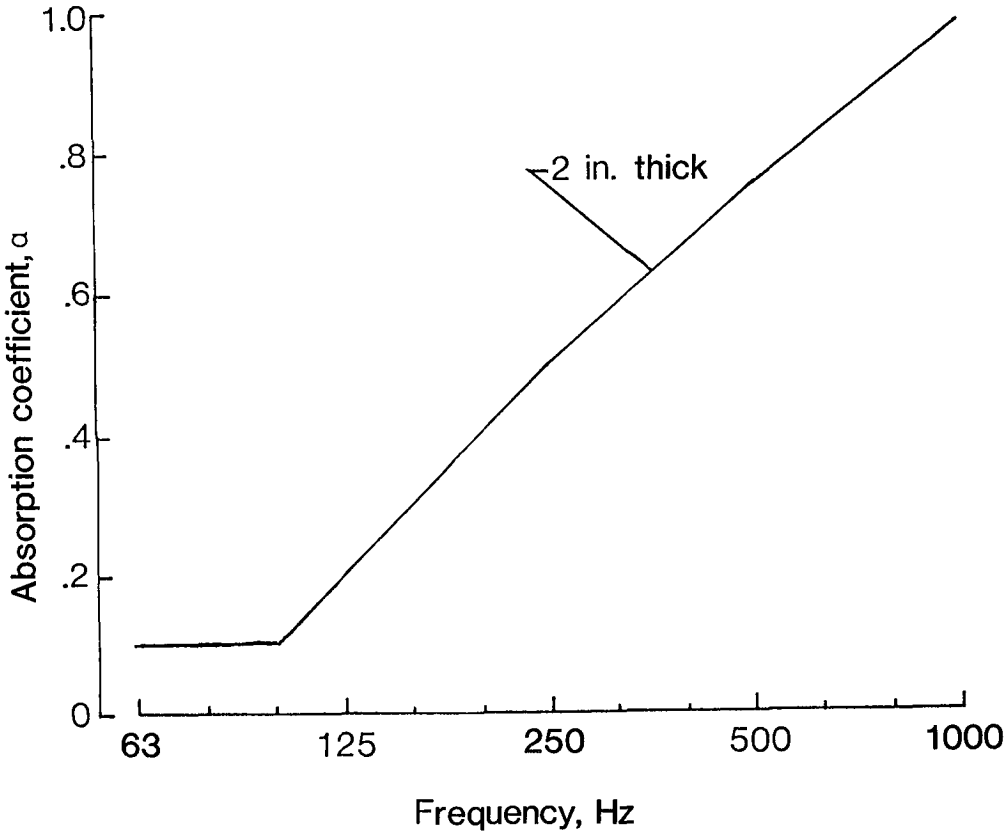

Figure 9.- Absorption coefficients for fiberglass used in equation (22).

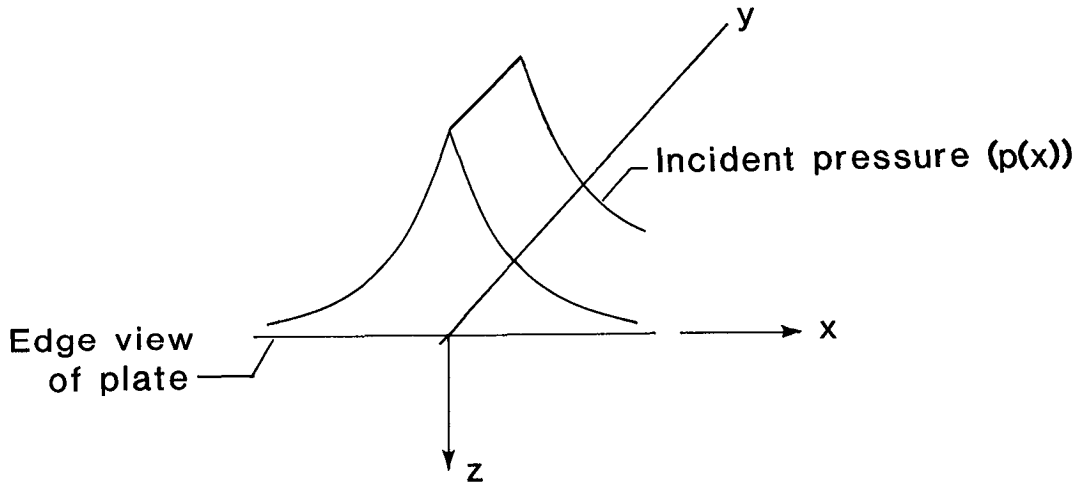

Figure 10.- Geometry for nonuniform incident pressure. Pressure is constant in y-direction; $p(x) = Pe^{-b|x|}$.

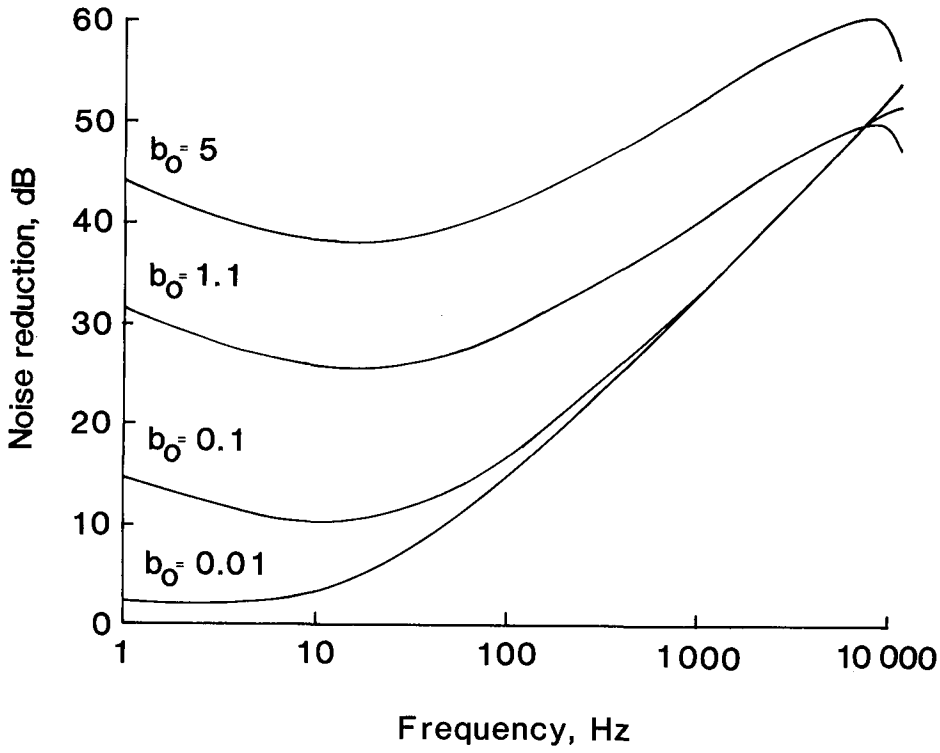

Figure 11.- Variation of calculated noise reduction with nondimensional source-plate parameter. $b_o = b/k_0$; $k_0 = 2\pi/\lambda_p = \sqrt[4]{m\omega^2/D}$.

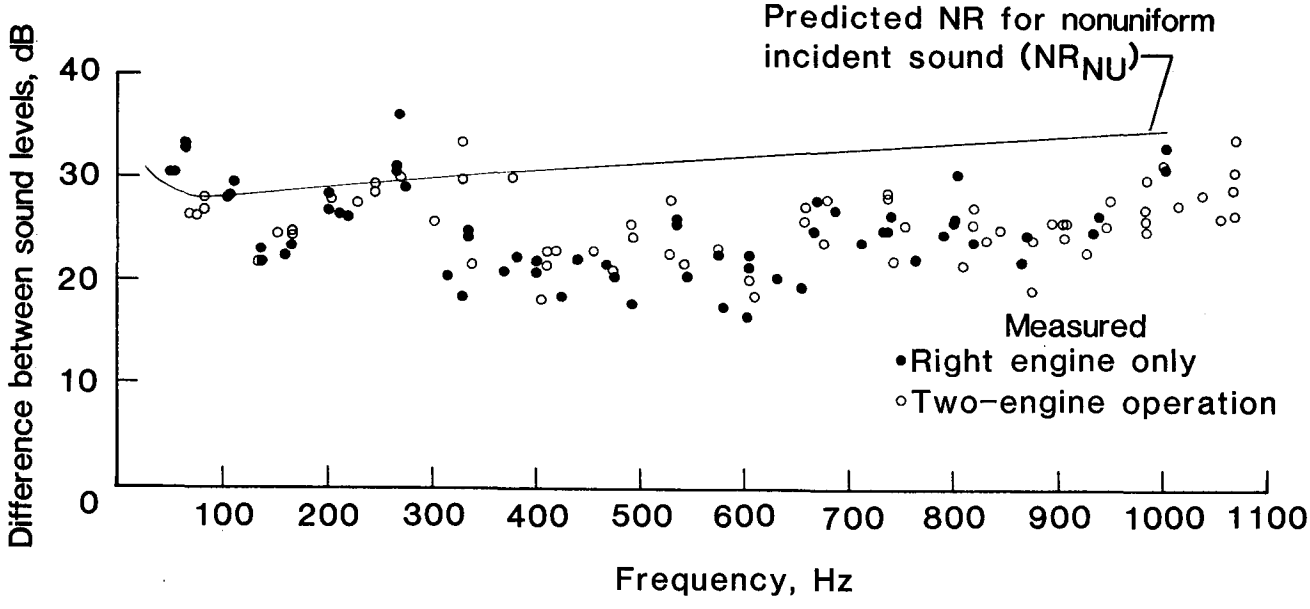

Figure 12.- Noise transmission from propeller test and nonuniform source calculation.

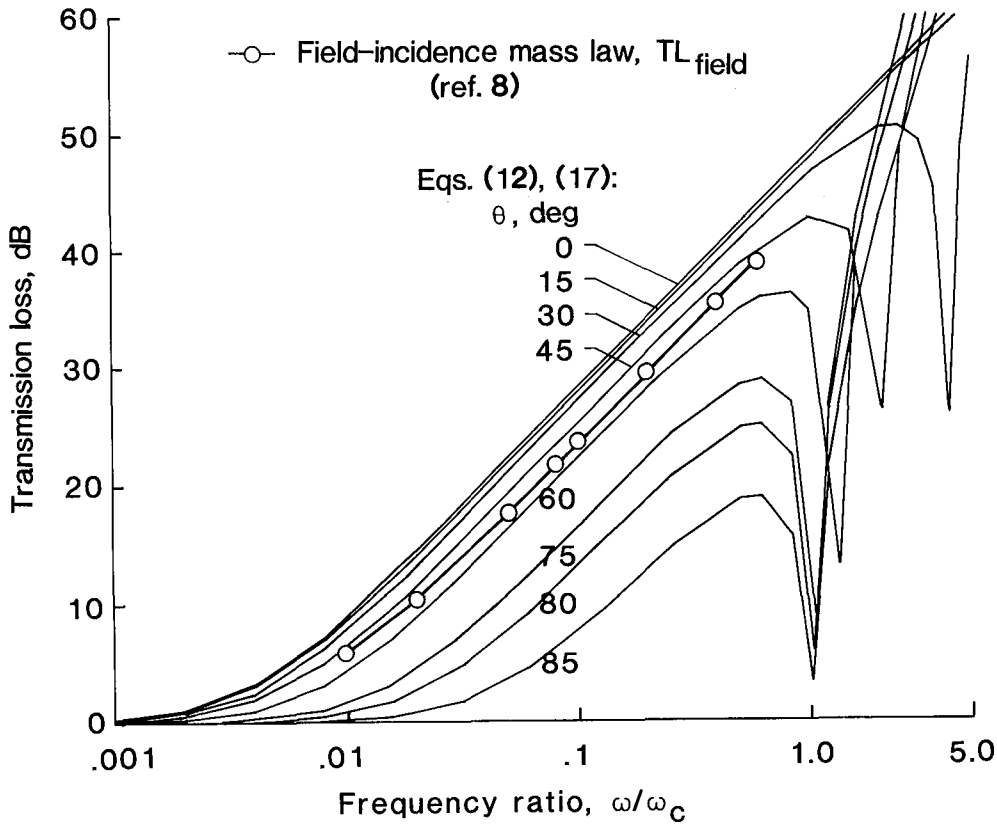

Figure 13.- Variation of transmission loss with frequency ratio for discrete and random incidence sound.

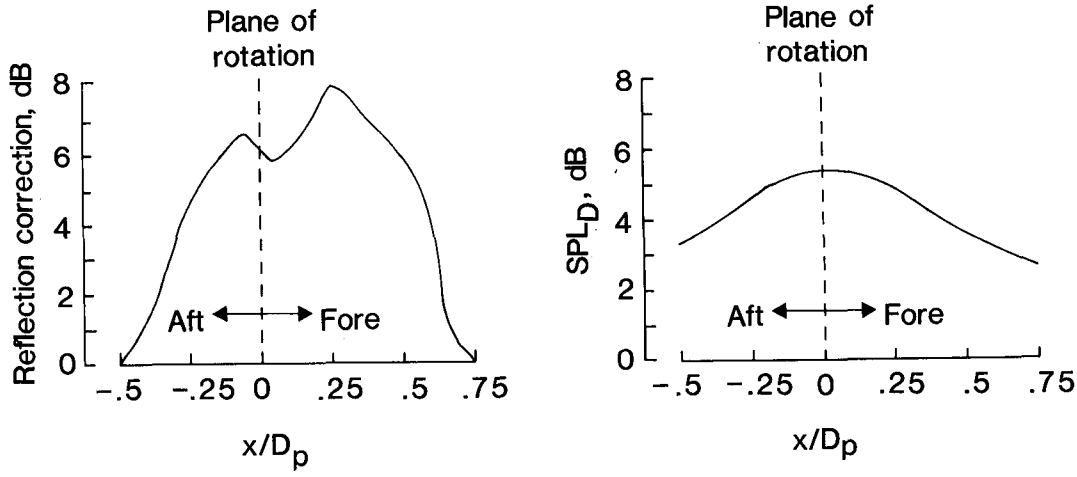

(a) Empirical curve from reference 9.

(b) Predicted curve using equation (20).

Figure 14.- Effect of reflecting surface in pressure field.

1. Report No.	2. Government Accession No.	3. Recipient's Catalog No.
NASA TP-2552		

4. Title and Subtitle	5. Report Date
Consideration of Some Factors Affecting Low-Frequency Fuselage Noise Transmission for Propeller Aircraft	April 1986
	6. Performing Organization Code 505-33-53-03
7. Author(s)	8. Performing Organization Report No.
John S. Mixson and Louis A. Roussos	L-15994
	10. Work Unit No.
9. Performing Organization Name and Address	
NASA Langley Research Center Hampton, VA 23665-5225	11. Contract or Grant No.
	13. Type of Report and Period Covered
12. Sponsoring Agency Name and Address	Technical Paper
National Aeronautics and Space Administration Washington, DC 20546-0001	14. Sponsoring Agency Code

15. Supplementary Notes

16. Abstract

Possible reasons for disagreement between measured and predicted trends of sidewall noise transmission at low frequency are investigated using simplified analysis methods. An analytical model combining incident plane acoustic waves with an infinite flat panel is used to study the effects of sound incidence angle, plate structural properties, frequency, absorption, and the difference between noise reduction and transmission loss. Analysis shows that these factors have significant effects on noise transmission but they do not account for the differences between measured and predicted trends at low frequencies. An analytical model combining an infinite flat plate with a normally incident acoustic wave having exponentially decaying magnitude along one coordinate is used to study the effect of a localized source distribution such as is associated with propeller noise. Results show that the localization brings the predicted low-frequency trend of noise transmission into better agreement with measured propeller results. This effect is independent of low-frequency stiffness effects that have been previously reported to be associated with boundary conditions.

17. Key Words (Suggested by Author(s))	18. Distribution Statement
Noise transmission Transmission loss Propeller noise	Unclassified - Unlimited Subject Category 71

19. Security Classif. (of this report)	20. Security Classif. (of this page)	21. No. of Pages	22. Price
Unclassified	Unclassified	26	A03

For sale by the National Technical Information Service, Springfield, Virginia 22161

NASA-Langley, 1986

National Aeronautics and
Space Administration
Code NIT-4

Washington, D.C.
20546-0001